relaxation times corresponding to the ionic relaxtion at 295 K have been estimated as mentioned in Table IV. These results confirm once more the electrostatic origin of the ion aggregation; the stability of large-size ionic aggregates is indeed inversely related to the cation radius or directly proportional to the electrostatic interaction forces. As pointed out by Eisenberg et al.[2] in ionomers and confirmed by us in HTP,[8] the polarity of the medium has a great influence on the ion aggregation, but it appears from this study that the ion content, the nature of the ion pair, and the mobility of the polymeric backbone—and especially the extent of entanglements for polymers above T_g—also have a significant influence. It results therefore that the ion aggregation in detectable domains is kinetically controlled, similarly to the glass transition in amorphous polymers, and it will be hazardous to assess when the ion-containing polymers are really studied in their state of thermodynamic equilibrium.

Some aspects of the ion aggregation in polymeric matrices are also to be outlined as challenges for further study. First, what is the mean size of the ionic aggregates just sufficient to detect an ionic relaxtion? Second, the large-size ionic aggregates are currently described as ionic clusters in ionomers,[1,15] but which is it in halato-telechelic polymers? In that respect, ordered structures with a lamellar character have been reported in some carboxylato-telechelic polybutadienes and seem to be favored by large-size cations such as Ba and K.[7]

Acknowledgment. We are indebted to UNIBRA (Brussels) and the "Service de la Programmation de la Politique Scientifique" for financial support and a fellowship (to G.B.). We are also grateful to G. Renders for skillful technical assistance.

References and Notes

(1) Eisenberg, A.; King, M. "Polymer Physics"; Stein, R. S., Ed.; Academic Press: New York, 1977; Vol. 2.
(2) Eisenberg, A.; Matsuura, H.; Tsutsui, T. *J. Polym. Sci., Polym. Phys. Ed.* **1980**, *18*, 479.
(3) Agarwal, P. K.; Makowski, H. S.; Lundberg, R. D. *Macromolecules* **1980**, *13*, 1679.
(4) Weiss, R. A.; Agarwal, P. K. *J. Appl. Polym. Sci.* **1981**, *26*, 449.
(5) Broze, G.; Jerome, R.; Teyssie, Ph. *Macromolecules* **1981**, *14*, 224.
(6) Broze, G.; Jerome, R.; Teyssie, Ph.; Marco, C. *Polym. Bull.* **1981**, *4*, 241.
(7) Broze, G.; Jerome, R.; Teyssie, Ph.; Gallot, B. *J. Polym. Sci., Polym. Lett. Ed.* **1981**, *19*, 415.
(8) Broze, G.; Jerome, R.; Teyssie, Ph. *Macromolecules* **1982**, *15*, 920.
(9) Broze, G.; Jerome, R.; Teyssie, Ph. *Macromolecules* **1982**, *15*, 1300.
(10) Broze, G.; Jerome, R.; Teyssie, Ph.; Marco, C. *Macromolecules* **1983**, *16*, 996.
(11) Broze, G.; Jerome, R.; Teyssie, Ph.; Marco, C. *J. Polym. Sci., Polym. Phys. Ed.*, to be published (Part VII).
(12) Otocka, E. P.; Hellman, M. Y.; Blyler, L. L. *J. Appl. Phys.* **1969**, *40*, 4221.
(13) Strobel, C. W. U.S. Patent 3 287 344, 1966.
(14) Personal communication of a reviewer.
(15) Eisenberg, A. *Contemp. Top. Polym. Sci.* **1979**, *3*, 231.

Investigation of Short-Chain Branches in Polyethylene by Pyrolysis-GCMS

M. A. Haney,*,† D. W. Johnston, and B. H. Clampitt*

Gulf Oil Chemicals Company, Polymer Research Center, Houston, Texas 77079.
Received October 18, 1982

ABSTRACT: A novel pyrolysis-hydrogenation-GCMS technique has been developed and applied to branched polyethylenes of both the high-pressure and low-pressure varieties. The unique features of the technique are pyrolysis at low temperatures (360 °C) and low extent of pyrolysis of the sample (approximately 2% volatilized). This yields a high percentage of pyrolysis products pertaining to the branch points. Study of model ethylene-α-olefin copolymers shows that the pyrolysis products from branch points can be predicted solely by consideration of the possible carbon-carbon scissions α and β to the branch points. The variety of products from high-pressure polyethylene, however, is greater than that expected simply from the branch-formation mechanism proposed by Roedel and Willbourn. An expanded polymerization scheme has been formulated that includes the occurrence of intramolecular 1,3 hydrogen transfers as well as intramolecular 1,5 hydrogen transfers in the formation of short-chain branches.

Introduction

The short-chain branches in high-pressure polyethylene (HPPE) have been studied for a long time because of their influence on the physical properties of the product and because of their significance to the free radical polymerization mechanism. Various instrumental techniques have been used to determine the type and number of short branches. These include (a) infrared spectroscopy,[1] (b) carbon-13 NMR,[2-7] (c) radiolysis-GC,[8-10] (d) pyrolysis-GC,[11-16] and (e) pyrolysis-GCMS.[17] These techniques have shown the presence of ethyl and *n*-butyl.

A theoretical mechanism for formation of short branches in the free-radical polymerization process was originally proposed by Roedel.[18] The growing polymer chain occasionally "back-bites" (intramolecular hydrogen transfer), producing a secondary radical site further down the chain.

$$\sim C-\overset{H}{C}-C-C-C-\dot{C} \longrightarrow \sim C-\dot{C}-C-C-C-C \quad (1)$$

The new radical site continues polymerization

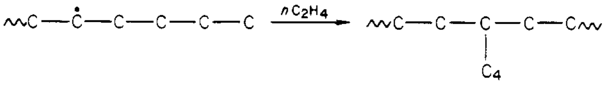

$$\sim C-\dot{C}-C-C-C-C \xrightarrow{nC_2H_4} \sim C-C-\underset{C_4}{C}-C-C\sim \quad (2)$$

The hydrogen abstraction was presumed to occur mostly on the fifth carbon as shown because this involves a sterically favored six-membered-ring intermediate. This mechanism, however, does not account for the other alkyl

---

[†] Present address: Gulf Oil Chemicals, Kingwood Technical Center, Kingwood, Texas 77339.

0024-9297/83/2216-1775$01.50/0

Table I
Properties of Polyethylenes in This Study

sample type	sample no.	density	MI at 190 °C	CH_3/1000 C[a]	C_2H_5/1000 C[a]
linear (control)	31069	0.9484	0.3	1.9	
copoly(4-methyl-1-pentene-ethylene)	31077	0.9264	0.1	24.0	
copoly(4-ethyl-1-octene-ethylene)	31075	0.9401	0.1	4.3	2.5
copoly(5-ethyl-1-nonene-ethylene)	31076	0.9273	0.2	18.0	8.5
copoly(1-butene-ethylene)	BR290	0.9310	6.1	24.2	22.2
copoly(1-butene-1-octene-ethylene)	BR217	0.9382	2.0	14.4	4.48
HPPE	1017	0.916	5.9	32.5	1.83
HPPE	2630T	0.933	1.3	6.78	4.17
HPPE	5503	0.923	1.9	25.8	3.29

[a] Obtained by infrared measurements after the manner of ref 1.

species observed, the large ethyl content. Therefore, Willbourn extended the Roedel mechanism by proposing that a second back-bite sometimes occurs after the addition of a single ethylene molecule.

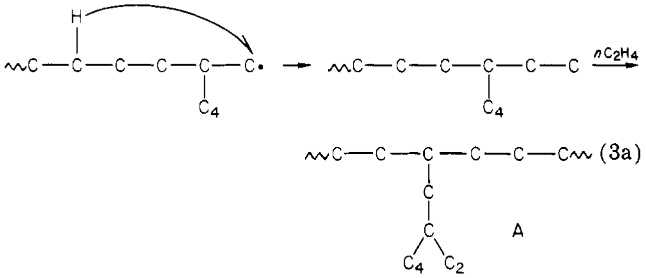

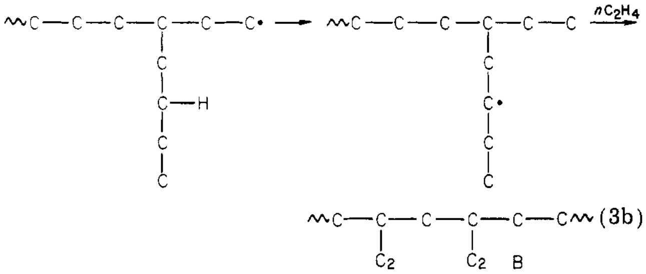

This mechanism, in conjunction with the single-back-biting mechanism, accounts for the observed presence of ethyl and *n*-butyl groups.

A notable aspect of the Willbourn–Roedel mechanism is that it requires an appreciable fraction of the chain branches to be branched also, e.g., 2-ethylhexyl (A). Direct experimental proof of the existence of these types of branches in HPPE is still lacking. Casey et al.[19] were able to infer their existence by comparing the melting points of HPPE with those of ethylene copolymers having linear branches. The melting points of HPPE samples were consistently higher than those of the linear branched copolymers of identical methyl content (as determined by IR absorption for all the polymers). They deduced that the methyl content of HPPE overestimates the number of branches, which is consistent with the presence of branched branches. Tirpak[20,21] measured the dichroism of the IR band of ethyl groups in HPPE and concluded that the ethyls were not attached to the backbone but to a branch near the backbone, as in 2-ethylhexyl (A), for example. Von Dohlen and Wilson[22] examined the low molecular weight oils taken from HPPE reactions and found branched alkenes whose structures were consistent with the Willbourn–Roedel mechanism.

The carbon-13 NMR studies of HPPE are inconclusive in regard to the presence of Willbourn branches. The earlier studies of Randall,[3] Dorman et al.,[2] Cudby and Bunn,[4] and Bovey[5] found only linear branches. Later work by Bowmer and O'Donnell[10] and by Mandelkern and co-workers[6,7] found evidence of Willbourn branches. Some questions remain, however, since Bowmer and O'Donnell claimed both Willbourn branch structure types (A and B) were found, whereas Mandelkern and co-workers could only confirm the presence of 1,3 ethyl pairs (B). The latter workers also found 1,2 ethyl pairs, which cannot be reconciled to the Willbourn–Roedel mechanism.

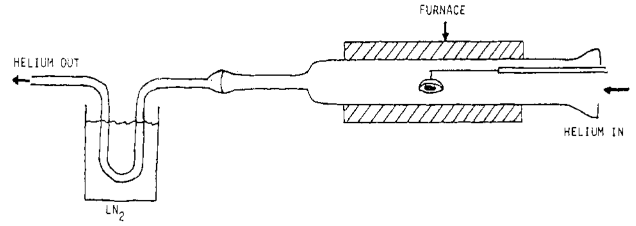

Figure 1. Apparatus for collection of pyrolysis products from TGA. Temperature = 360 °C, flow rate = 60 mL/min, sample weight = 15 mg, sample weight loss = 2%.

Numerous pyrolysis studies[11-17] have focused on the linear branches in HPPE without finding Willbourn-type branches. This may be due to the fact that these investigators were not specifically looking for them. Indeed, they may not have been aware of the Willbourn mechanism since it was not mentioned in any of the papers.

Accordingly, we have made a pyrolysis–GCMS study of HPPE with the express purpose of searching for branches indicative of the Willbourn mechanism. The approach differs from previous pyrolysis studies in two important aspects: (a) Linear polyethylenes containing Willbourn-type branches introduced by copolymerization have been studied. (b) The samples have been pyrolyzed at low temperatures with only the first 2% of volatiles analyzed in order to maximize the scission of branches from the polymer chain while minimizing chain scission. This makes it easier to sort out those pyrolysis products that result from branches. Hydrogenation of the pyrolysis products before gas chromatography has also been employed to simplify the chromatogram and make it easier to obtain identification of all the products by mass spectrometry.

Experimental Section

Samples. Descriptions and properties of the samples pyrolyzed are shown in Table I. The copolymers were synthesized by the low-pressure Ziegler process and should be essentially linear polyethylenes that contain branches introduced by the comonomers. The methyl and ethyl group determinations by IR confirm that this is the case. The HPPE samples are standard Gulf products made by a conventional autoclave process. No comonomers were used in the production of the HPPE samples so that all branching is purely the result of the free radical process.

Pyrolysis. In order to meet the conditions of low temperature and controlled evolution of volatiles, the samples were pyrolyzed on a thermogravimetric analyzer (TGA). This allows close control

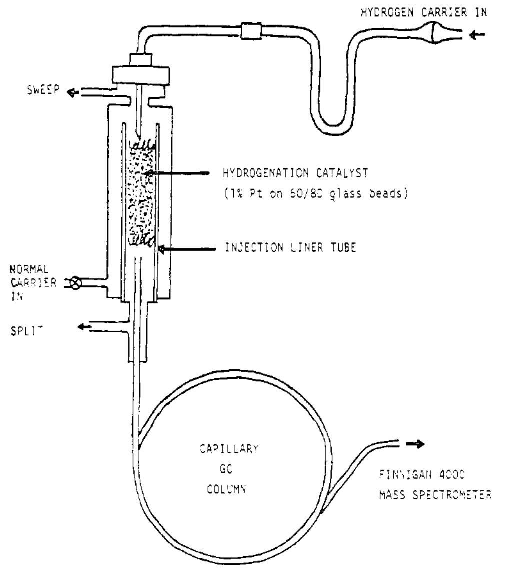

Figure 2. Apparatus for hydrogenation of pyrolysis products. GC operating conditions: injection temperature, 225 °C; column, SS capillary, 100 m × 0.25 mm, OV-101, column temperature, 30 °C (5 min) → 90 °C (1 min), 190 °C at 5 °C/min. Mass spectrometer operating conditions: EI, 70 eV; mass scan, 35–200 amu, 1 scan/s.

of temperature and weight loss. A schematic of the pyrolysis and volatile collection apparatus is shown in Figure 1.

The volatiles swept from the TGA were trapped in the copper tubing chilled in a liquid nitrogen bath. Operating conditions of the TGA were as follows: carrier gas, helium at 60 mL/min; temperature program, heated from ambient to 360 °C at 10 °C/min and then held at 360 °C; sample weight, 15–30 mg. The liquid nitrogen trap was connected when the sample began to lose weight, which occurred at about 350 °C for most of the samples. Trapping continued at the 360 °C limit until 2% of the original sample weight had volatilized. This required anywhere from 15 min to an hour, depending on the sample. The trap was removed from the TGA and placed in the carrier gas line of the GC.

GCMS. The instrument used was a Finnigan Model 4023, equipped with a capillary GC column and an Incos data system. The mass spectrometer was operated in the conventional EI mode at 70 eV, with mass scan from 35 to 200 amu at a rate of one scan per second. Except where noted in the text, all compounds were identified by computer search of the National Bureau of Standards Mass Spectral Compilation Library provided with the Incos system.

The GC column was a stainless steel capillary 100 m × 0.25 mm i.d., wall coated with OV-101 by Analabs Inc. Theoretical plate count was approximately 350 000. Linear flow rate through the column was approximately 30 cm/s, with a split flow rate of 50 mL/min. Column temperature was held initially at ambient for 5 min, increased rapidly to 90 °C and held for 1 min, and programed at 5 °C/min to 190 °C and held.

The volatiles were hydrogenated in the injector of the GC as shown in Figure 2. A catalyst consisting of 1% (w/w) platinum on 60/80 glass beads was placed in the glass liner of the injector. The injector temperature was 225 °C. Hydrogen was used as the GC carrier gas.

It was found that peak spreading of the more volatile components could be prevented by rigging a temporary liquid nitrogen trap on the head of the GC column to retrap the volatiles as they are released from the collection trap. This was accomplished by coiling about 1 ft of the capillary into a loop and placing this loop into a Dewar flask of liquid nitrogen. As soon as the collection trap was fully warmed with a heat gun, the liquid nitrogen trap was removed and elution was begun.

Results and Discussion

Linear Polyethylene. Figure 3 shows the pyrogram of the unbranched polyethylene sample (HDPE 31069). As expected, normal alkanes are the predominant products, their intensities increasing systematically in the C_3 to C_7 range and then leveling off at C_8 and above. Minor amounts of cyclic alkanes are also found. These have been found by other workers. Significantly, there is an absence of branched alkanes.

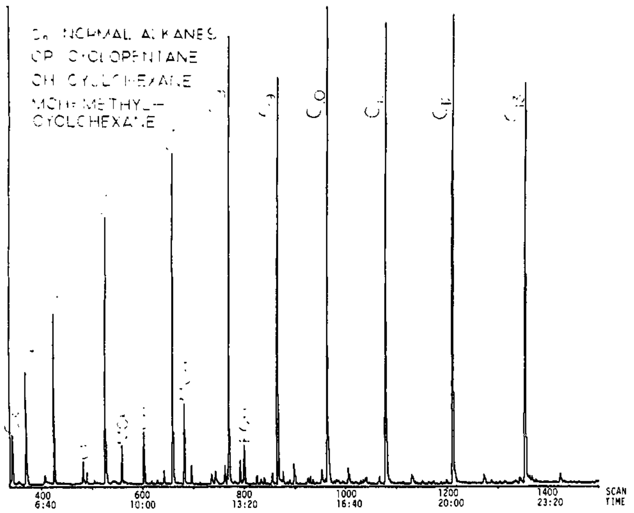

Figure 3. Pyrogram of linear (control) polyethylene.

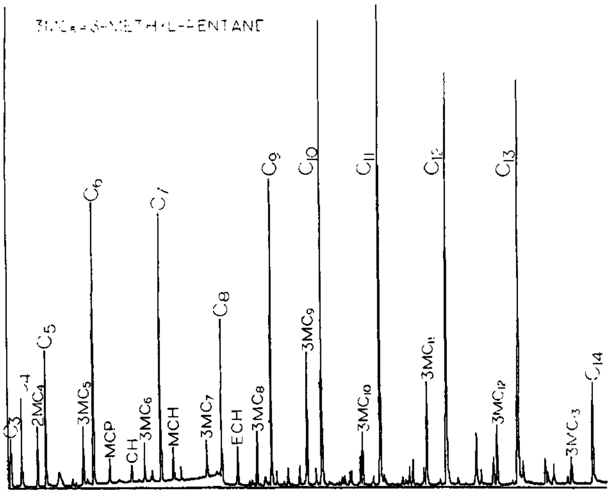

Figure 4. Pyrogram of ethylene-1-butene copolymer.

Linear Polyethylenes with Linear Branches. These polymers have been extensively studied by pyrolysis.[11-17] The general conclusion is that an isolated branch of *n* carbons pyrolyzes by the following process:

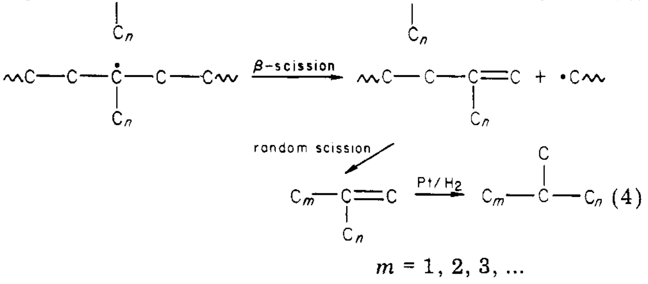

$$\sim C-C-\underset{\displaystyle C_n}{\underset{|}{C}}-C-C\sim \xrightarrow{R\cdot} \sim C-C-\underset{\displaystyle C_n}{\underset{|}{\dot{C}}}-C-C-C\sim + RH$$

$$\sim C-C-\underset{\displaystyle C_n}{\underset{|}{\dot{C}}}-C-C\sim \xrightarrow{\beta\text{-scission}} \sim C-C-\underset{\displaystyle C_n}{\underset{|}{C}}{=}C + \cdot C\sim$$

$$\xrightarrow{\text{random scission}} C_m-\underset{\displaystyle C_n}{\underset{|}{C}}{=}C \xrightarrow{Pt/H_2} C_m-\overset{\displaystyle C}{\overset{|}{C}}-C_n \quad (4)$$

$$m = 1, 2, 3, ...$$

As shown, the olefin product is hydrogenated in the present experiment to give methylalkanes. These characteristic methylalkanes, then, should be clearly visible in the pyrograms of ethylene copolymerized with 1-butene (Figure 4) and 1-butene-1-octene (Figure 5). These pyrograms, in fact, show the characteristic 3-methylalkanes formed from ethyl branches (*n* = 2 in mechanism 4).

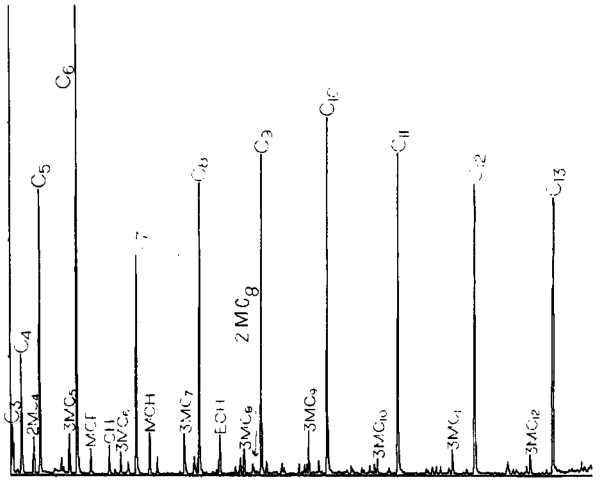

Figure 5. Pyrogram of ethylene–1-butene–1-octene copolymer.

Moreover, the series of 3-methylalkanes are relatively consistent in intensity. However, the hexyl branches on the octene copolymer (Figure 5) do not yield nearly as much methylalkanes as do the short ethyl branches. Only a small amount of $2MC_8$ is visible in the octene copolymer program. The rest of the series (except for the $3MC_9$, which is also formed from the ethyl branches of the butene comonomer) is not visibly present.

The octene copolymer pyrogram does, however, show much more pentane and hexane than would be expected from random scission of the chain. These products presumably come from α- and β-scissions on the hexyl branch, rather than on the chain. The mechanisms are as follows:

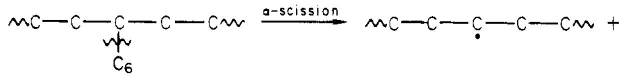

$$\sim C-C-\underset{\underset{C_6}{\wr}}{C}-C-C\sim \xrightarrow{\alpha\text{-scission}} \sim C-C-\underset{\bullet}{C}-C-C\sim + \bullet C_6 \tag{5}$$

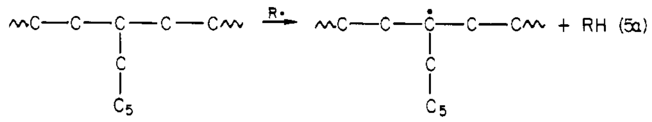

$$\sim C-C-\underset{\underset{C_5}{|}}{\underset{|}{C}}\!\!\!\!\!\!\!\quad\underset{}{}\!-C-C\sim \xrightarrow{R\bullet} \sim C-C-\overset{\bullet}{\underset{\underset{C_5}{|}}{\underset{|}{C}}}-C-C\sim + RH \tag{5a}$$

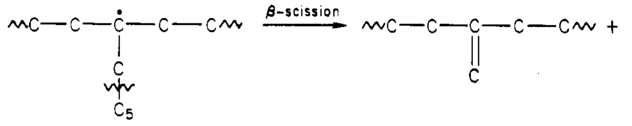

$$\sim C-C-\overset{\bullet}{\underset{\underset{C_5}{\wr}}{\underset{|}{C}}}-C-C\sim \xrightarrow{\beta\text{-scission}} \sim C-C-\underset{C}{\underset{\|}{C}}-C-C\sim + \bullet C_5 \tag{6}$$

These types of products have been postulated in previous pyrolysis studies[11,14] but were not specifically observed due to the high concentration of linear alkanes coming from the chain degradation. The pyrolysis technique used in the present study emphasizes branch scission sufficiently that the linear branch fragments arising from mechanisms 5 and 6 can be observed in excess of the linear fragments arising from chain scission.

No attempt was made to look for the expected linear branch products of the 1-butene copolymer. Ethane and methane cannot be detected by the mass spectrometer, which operates in the usual mass range above the air and water background peaks. They would also not be trapped by the liquid nitrogen trap.

Finally, there is also evidence in several of the pyrograms that the C_3 and C_4 hydrocarbons are not perfectly trapped either. Presumably this is due mainly to the transfer of the pyrolysates from the TGA to the GCMS. In the face of this evidence no attempt was made to study an ethylene–hexene copolymer, which would not have supplied totally reliable data. Nevertheless, the C_4 in the HPPE's (discussed below) is obviously enhanced over its intensity from any of the model copolymers studied. Thus mechanism 5, and thus probably also mechanism 6, does operate for *n*-butyl branches. The expected $5MC_n$ series, from mechanism 4, is also evident in the HPPE pyrograms, and has been noted by other investigators.[17] There is no evidence from this experiment or from the literature to suggest that other mechanisms might also be in operation.

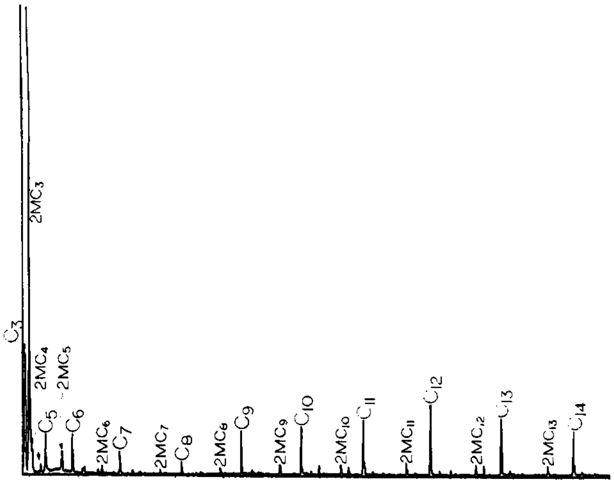

Figure 6. Pyrogram of ethylene–4-methyl-1-pentene copolymer.

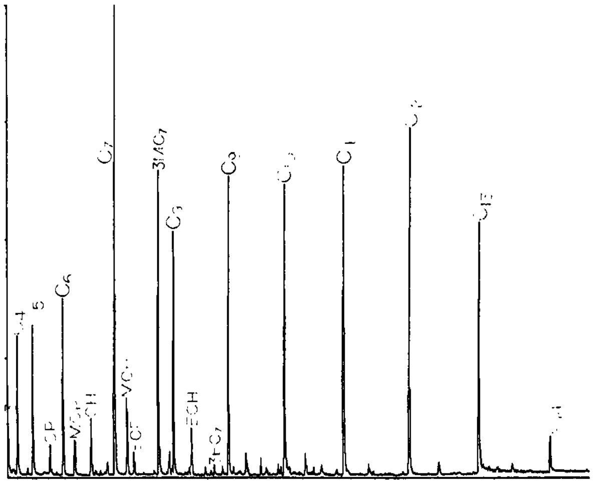

Figure 7. Pyrogram of ethylene–4-ethyl-1-octene copolymer.

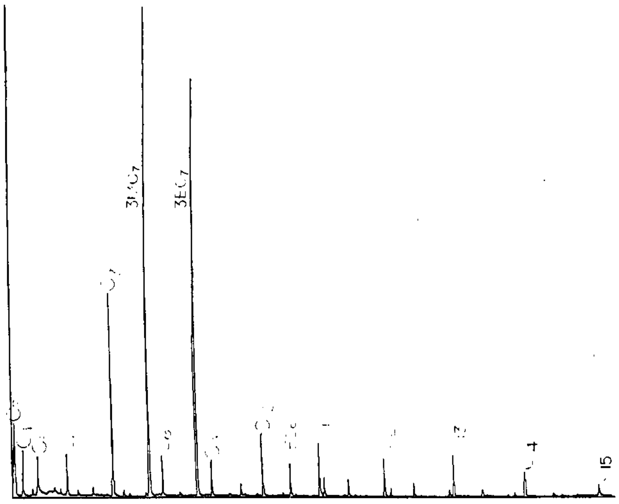

Figure 8. Pyrogram of ethylene–5-ethyl-1-nonene copolymer.

Linear Polyethylene with Branched Branches. The pyrograms of polyethylene containing isobutyl branches, 2-ethylhexyl branches, and 3-ethylheptyl branches are shown in Figures 6–8, respectively. The predominant mode of scission is *along the branch* α and β to either the branch point on the chain or the branch point on the branch. This is best illustrated by the 3-ethylheptyl branch of Figure 8. The obvious branch products are heptane, 3-methylheptane, and 3-ethylheptane, formed by the following mechanisms:

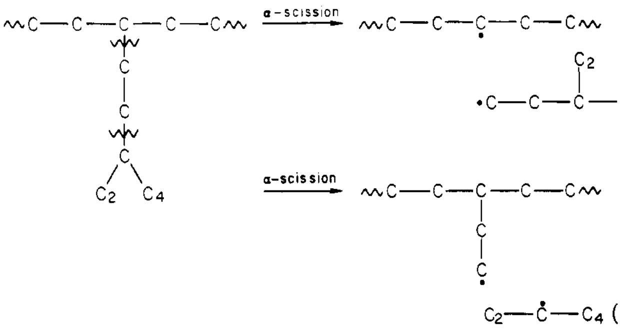
(7)

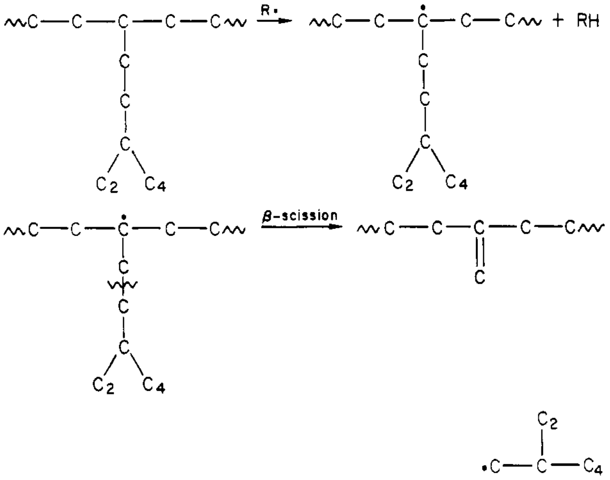
(8)

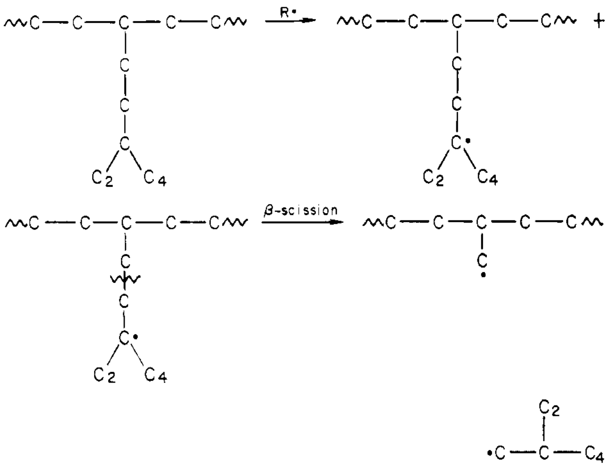
(9)

The free radical pyrolysates in each case can either lose or abstract hydrogen (intermolecular) to form the alkene or alkane. Irrespective, only alkanes appear in the chromatograms due to the Pt/H_2 hydrogenation that takes place in the injection port of the GC.

Similar mechanisms account for propane and isobutane as the major products from the pyrolysis of 4-methyl-1-pentene copolymer in Figure 6 and for heptane and 3-methylheptane from the 4-ethyl-1-octene copolymer of Figure 7.

Minor amounts of other scission products are also present in the 4-methyl-1-pentene copolymer; for instance, there are $2MC_5$, $2MC_6$, $2MC_7$, etc. These arise from α-scission along with chain at the branch point on the chain:

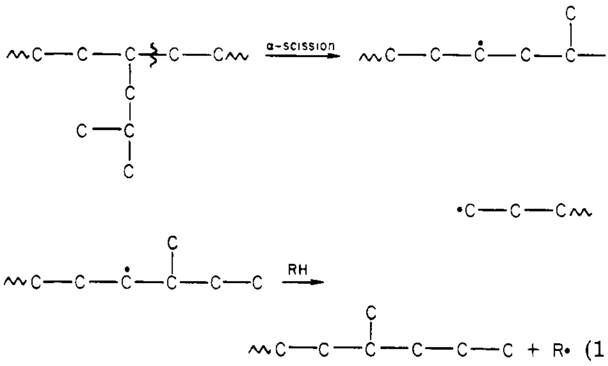
(10a)

This chain end can then undergo random scission along the chain to form the series of 2-methylalkanes. The same mechanism operating on the 4-ethyl-1-octene copolymer and the 5-ethyl-1-nonene copolymer will yield the following chain end from both polymers:

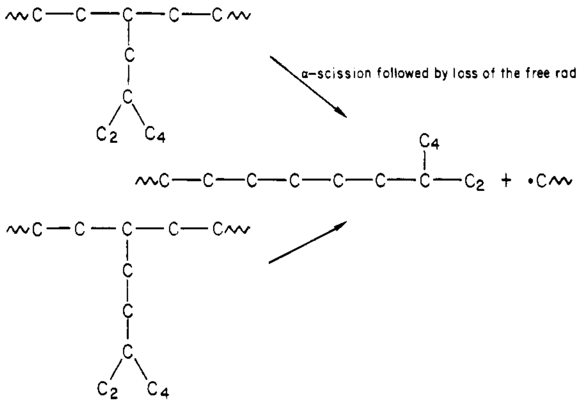
(10b)

The series of products from random scission of this end group would be $3MC_7$, $3EC_7$, $4EC_8$, $5EC_9$, etc. Only very small amounts of these compounds were present in the 4-ethyl-1-octene pyrogram (Figure 7) and none are visible in the 5-ethyl-1-nonene pyrogram (Figure 8). Finally, there is also the possibility of free radical formation at the chain branch point followed by β-scission, similar to mechanism 4:

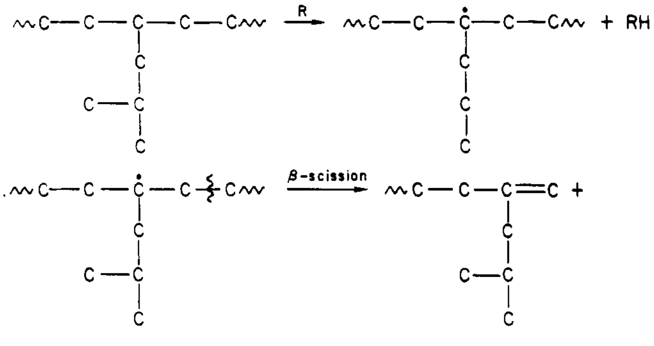
(11)

Following random scission and hydrogenation, a series of products would be formed of the type

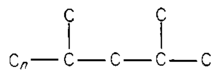
I, $n = 1, 2, 3, \ldots$

The same mechanism operating on the 4-ethyl-1-octene copolymer would produce alkanes of the type

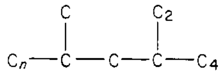
II, $n = 1, 2, 3, \ldots$

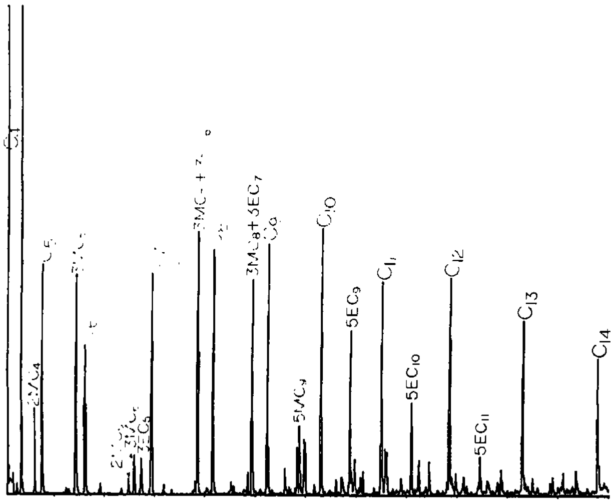

Figure 9. Pyrogram of HPPE 1017.

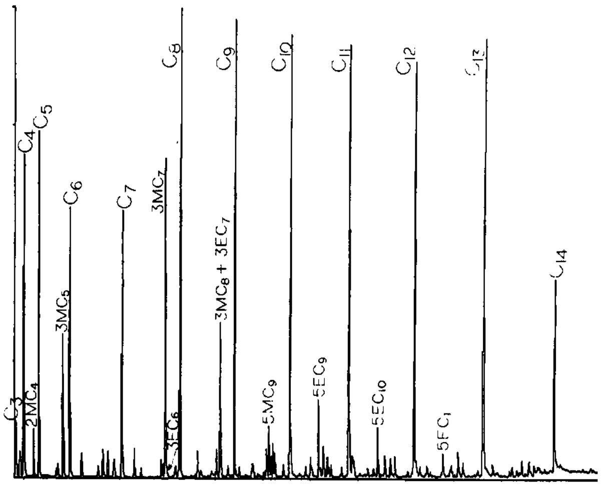

Figure 10. Pyrogram of HPPE 2630.

And the 5-ethyl-1-nonene copolymer would produce the series

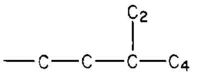

$$\mathrm{C}_n-\overset{\mathrm{C}}{\overset{|}{\mathrm{C}}}-\mathrm{C}-\mathrm{C}-\overset{\mathrm{C_2}}{\overset{|}{\mathrm{C}}}-\mathrm{C_4}$$

III, $n = 1, 2, 3, \ldots$

None of these series are present in the chromatograms.

Thus there is a hierarchy of preferred modes of scission. Scission along the branch α and β to branch points is, as said before, predominant. Next comes along the chain β to the branch point on the chain. Finally, there is no evidence that scission along the chain β to the branch point on the chain occurs at all. This is in line with the observation that there are no 7-methylalkanes visible in the ethylene–octene copolymer pyrogram (with the exception of a small amount of $2MC_8$). Possibly the length of the branch plays some factor in the rates of the competing mechanisms.

High-Pressure Polyethylene. It appears from the above results that Willbourn-type branches should be easily detected in the pyrograms of HPPE even if they are present only in low concentrations. The pyrograms of three HPPE samples in Figures 9–11 indeed show the presence of branched products that are expected on the basis of the Willbourn theory. Moreover, all three pyrograms are qualitatively identical.

The large excess of $3MC_7$ appears to be immediate evidence of 2-ethylhexyl branches (type A). There is also a small amount of 2,4-diethylpentane, which would be formed from Willbourn branches of type B by the following mechanism:

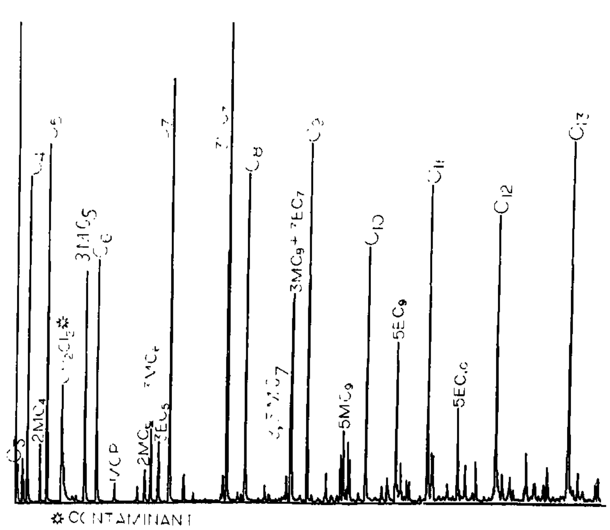

Figure 11. Pyrogram of HPPE 5503.

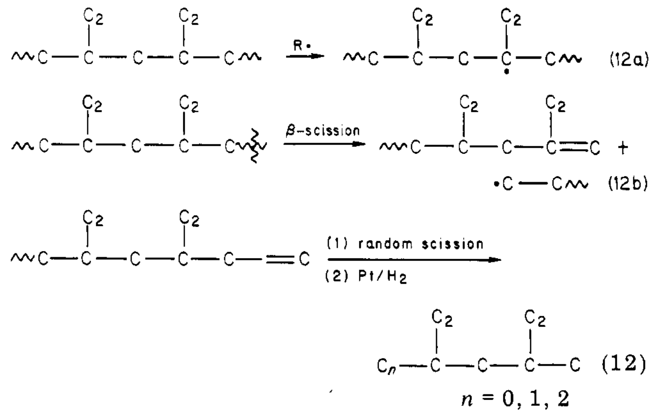

$$\sim\mathrm{C}-\overset{\mathrm{C_2}}{\overset{|}{\mathrm{C}}}-\mathrm{C}-\overset{\mathrm{C_2}}{\overset{|}{\mathrm{C}}}-\mathrm{C}\sim \xrightarrow{\mathrm{R}\cdot} \sim\mathrm{C}-\overset{\mathrm{C_2}}{\overset{|}{\mathrm{C}}}-\mathrm{C}-\underset{\bullet}{\overset{\mathrm{C_2}}{\overset{|}{\mathrm{C}}}}-\mathrm{C}\sim \quad (12a)$$

$$\sim\mathrm{C}-\overset{\mathrm{C_2}}{\overset{|}{\mathrm{C}}}-\mathrm{C}-\overset{\mathrm{C_2}}{\overset{|}{\mathrm{C}}}-\mathrm{C}\wr\sim \xrightarrow{\beta\text{-scission}} \sim\mathrm{C}-\overset{\mathrm{C_2}}{\overset{|}{\mathrm{C}}}-\mathrm{C}-\overset{\mathrm{C_2}}{\overset{|}{\mathrm{C}}}=\mathrm{C} + \cdot\mathrm{C}-\mathrm{C}\sim \quad (12b)$$

$$\sim\mathrm{C}-\overset{\mathrm{C_2}}{\overset{|}{\mathrm{C}}}-\mathrm{C}-\overset{\mathrm{C_2}}{\overset{|}{\mathrm{C}}}-\mathrm{C}-\!=\mathrm{C} \xrightarrow[\text{(2) Pt/H}_2]{\text{(1) random scission}} \mathrm{C}_n-\overset{\mathrm{C_2}}{\overset{|}{\mathrm{C}}}-\mathrm{C}-\overset{\mathrm{C_2}}{\overset{|}{\mathrm{C}}}-\mathrm{C} \quad (12)$$

$n = 0, 1, 2$

2,4-Diethylpentane is then the second member of the above series (the first member is $3MC_7$).

However, there is a much greater variety of branched products in the pyrograms than was expected from the study of copolymers with introduced branches just discussed. Moreover, some peaks, in particular that of $3MC_5$, are much more prominent than can be readily explained. From the discussion thus far, $3MC_5$ can only be formed from ethyl branches. The only source of ethyl branches would be the 1,3 ethyl pairs, and the familiar 3-methylalkanes would be formed by a variation of mechanism:

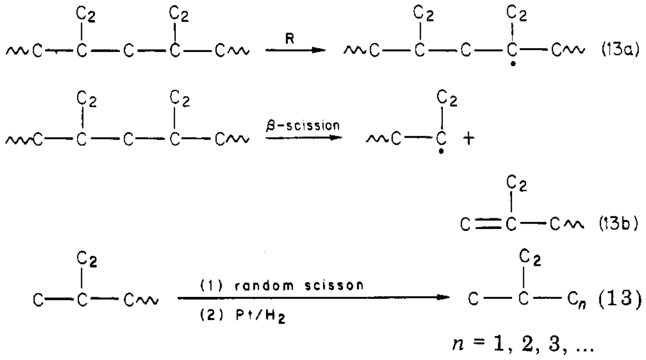

$$\sim\mathrm{C}-\overset{\mathrm{C_2}}{\overset{|}{\mathrm{C}}}-\mathrm{C}-\overset{\mathrm{C_2}}{\overset{|}{\mathrm{C}}}-\mathrm{C}\sim \xrightarrow{\mathrm{R}} \sim\mathrm{C}-\overset{\mathrm{C_2}}{\overset{|}{\mathrm{C}}}-\mathrm{C}-\underset{\bullet}{\overset{\mathrm{C_2}}{\overset{|}{\mathrm{C}}}}-\mathrm{C}\sim \quad (13a)$$

$$\sim\mathrm{C}-\overset{\mathrm{C_2}}{\overset{|}{\mathrm{C}}}-\mathrm{C}-\overset{\mathrm{C_2}}{\overset{|}{\mathrm{C}}}-\mathrm{C}\sim \xrightarrow{\beta\text{-scission}} \sim\mathrm{C}-\underset{\bullet}{\overset{\mathrm{C_2}}{\overset{|}{\mathrm{C}}}} + \mathrm{C}=\overset{\mathrm{C_2}}{\overset{|}{\mathrm{C}}}-\mathrm{C}\sim \quad (13b)$$

$$\mathrm{C}-\overset{\mathrm{C_2}}{\overset{|}{\mathrm{C}}}-\mathrm{C}\sim \xrightarrow[\text{(2) Pt/H}_2]{\text{(1) random scisson}} \mathrm{C}-\overset{\mathrm{C_2}}{\overset{|}{\mathrm{C}}}-\mathrm{C}_n \quad (13)$$

$n = 1, 2, 3, \ldots$

In fact, this mechanism would be favored over (12) thermodynamically since a secondary free radical is left after β-scission rather than a primary free radical. Nevertheless, each peak in this series should be of approximately equal

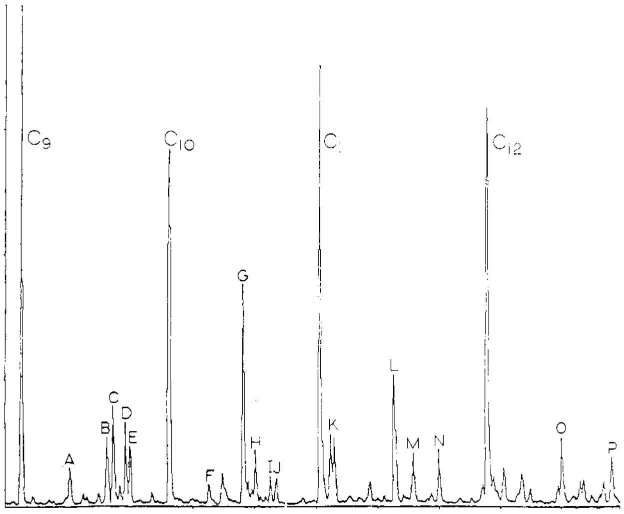

Figure 12. Expanded portion of pyrogram of HPPE 5503.

intensity as found with the polyethylenes with linear branches. Yet $3MC_5$ is clearly 3 or 4 times more intense in each pyrogram than the other members of this series.

In order to explain the new peaks and the anomalous intensity of the $3MC_5$ peak, it is necessary first of all to list all of the compounds identified in the pyrograms. Up to C_{10}, virtually all of the peaks are identified by library spectral matching. Beyond C_{10}, many of the peaks can still be identified by comparison of the relative retention times and mass spectra with those of lower homologues. Thus, the following homologous series can be determined:

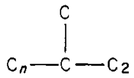
$\mathrm{C_{\mathit{n}}-\overset{C}{\overset{|}{C}}-C_2}$

IV, $n = 1, 2, 3, \ldots$

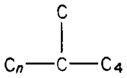
$\mathrm{C_{\mathit{n}}-\overset{C}{\overset{|}{C}}-C_4}$

V, $n = 1, 2, 3, \ldots$

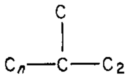
$\mathrm{C_{\mathit{n}}-\overset{C}{\overset{|}{C}}-C_2}$

VI, $n = 1, 2, 3, \ldots$

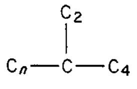
$\mathrm{C_{\mathit{n}}-\overset{C_2}{\overset{|}{C}}-C_4}$

VII, $n = 1, 2, 3, \ldots$

There is also apparent evidence that another series exists from mechanism 12, and this will be called series VIII:

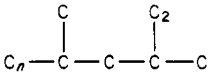
$\mathrm{C_{\mathit{n}}-\overset{C}{\overset{|}{C}}-C-\overset{C_2}{\overset{|}{C}}-C}$

VIII, $n = 1, 2, 3, \ldots$

This series offers an explanation of some of the heavier hydrocarbons that remain unidentified but not all of them. For convenience, the region of the pyrogram of PE5503 (Figure 11) containing these heavier unidentified peaks is shown in expanded form in Figure 12. The branched peaks are numbered in the pyrogram and identified in Table II. Before discussing these heavier hydrocarbons further, however, we make some comments on the series already identified. Series IV and V are quite familiar and obviously originate from ethyl and butyl branches, respectively. The intensity of the series VII peaks is somewhat greater than expected from the branched-branch copolymer study but they can be formed from 2-ethylhexyl branches of type A via mechanism 10, as a competing mechanism to α-scission on the branch. However, except for $3MC_5$ (from the 1,3 ethyl pairs) there is no branch structure encountered thus far to explain series VI.

In order to account for this series, a new polymerization mechanism is required. From the paper by Von Dohlen and Wilson[22] on the investigation of low molecular weight oils in HPPE, an enlarged scheme of polymerization mechanisms has been formulated that includes the occurrence of 1,3 intramolecular hydrogen transfer as well as of 1,5 intramolecular hydrogen transfer:

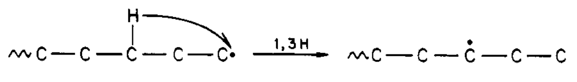
$\mathrm{\sim C-C-\overset{H}{\overset{|}{C}}-C-\dot{C}\xrightarrow{1,3H}\sim C-C-\dot{C}-C-C}$ (14)

This scheme, shown in Scheme I, was formulated on the basis of the following three assumptions: (1) Primary free radicals may undergo intramolecular hydrogen transfer either as 1,3H or 1,5H. Of course, they can also continue to react with monomer.

Table II
Labeled Peaks in Expanded Portion of Pyrogram of HDPE 5503

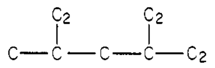 $\mathrm{C-\overset{C_2}{\overset{|}{C}}-C-\overset{C_2}{\overset{|}{C}}-C_2}$ A[a]	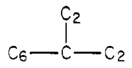 $\mathrm{C_6-\overset{C_2}{\overset{|}{C}}-C_2}$ I[a]
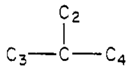 $\mathrm{C_3-\overset{C_2}{\overset{|}{C}}-C_4}$ B[a]	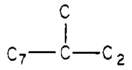 $\mathrm{C_7-\overset{C}{\overset{|}{C}}-C_2}$ J[a]
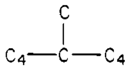 $\mathrm{C_4-\overset{C}{\overset{|}{C}}-C_4}$ C	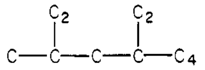 $\mathrm{C-\overset{C_2}{\overset{|}{C}}-C-\overset{C_2}{\overset{|}{C}}-C_4}$ K[a]
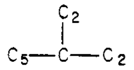 $\mathrm{C_5-\overset{C_2}{\overset{|}{C}}-C_2}$ D[a]	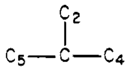 $\mathrm{C_5-\overset{C_2}{\overset{|}{C}}-C_4}$ L[a]
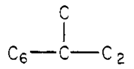 $\mathrm{C_6-\overset{C}{\overset{|}{C}}-C_2}$ E	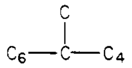 $\mathrm{C_6-\overset{C}{\overset{|}{C}}-C_4}$ M[a]
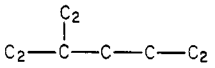 $\mathrm{C_2-\overset{C_2}{\overset{|}{C}}-C-C-C_2}$ F[a]	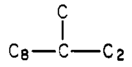 $\mathrm{C_8-\overset{C}{\overset{|}{C}}-C_2}$ N[a]
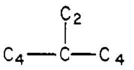 $\mathrm{C_4-\overset{C_2}{\overset{|}{C}}-C_4}$ G[a]	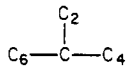 $\mathrm{C_6-\overset{C_2}{\overset{|}{C}}-C_4}$ O[a]
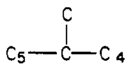 $\mathrm{C_5-\overset{C}{\overset{|}{C}}-C_4}$ H	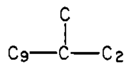 $\mathrm{C_9-\overset{C}{\overset{|}{C}}-C_2}$ P[a]

[a] Structure interpreted from mass spectrum.

Scheme I

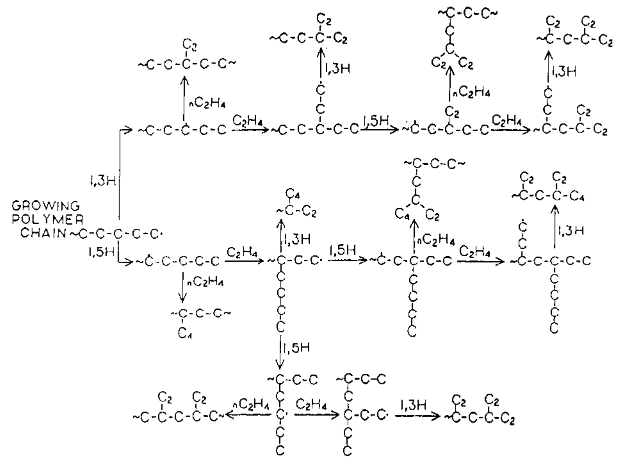

(2) Secondary free radicals formed by intramolecular hydrogen transfer undergo addition of one ethylene molecule to create a primary free radical again. As before, this free radical may undergo 1,3 or 1,5 hydrogen transfer or continue polymerization.

(3) Tertiary free radicals are formed only by 1,3 hydrogen transfer. It is assumed that these free radicals are prevented by both thermodynamic and steric considerations from undergoing either intramolecular hydrogen transfer of ethylene addition. They terminate eventually by intermolecular hydrogen transfer from polymerization terminators. Von Dohlen and Wilson[22] pointed out that scission of a tertiary free radical is also a likely fate. However, this does not produce polymer branches, but branched low molecular weight species.

This scheme adds two new series:

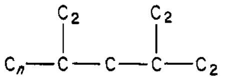

$C_n\text{—}\overset{C_2}{C}\text{—}C\text{—}\overset{C_2}{C}\text{—}C_2$

IX, $n = 1, 2, 3, \ldots$

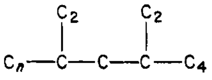

$C_n\text{—}\overset{C_2}{C}\text{—}C\text{—}\overset{C_2}{C}\text{—}C_4$

X, $n = 1, 2, 3, \ldots$

These two series, like series VI, have not before been predicted, yet they readily explain the presence of the unidentified higher molecular weight species. As with series VIII, positive correlation of the individual members of these series with the unidentified peaks in the chromatograms was deemed infeasible since none of them are readily or cheaply available. However, the spectra are still available for investigation at any time in the future.

Taking the scheme further, as well as predicting all of the indentified compounds in the pyrograms and offering identities for the unidentified compounds, it also offers an explanation for the observed excess of $3MC_5$. This excess derives from the fact that it is the favored scission product of several of the branches and branched-chain end groups, e.g.

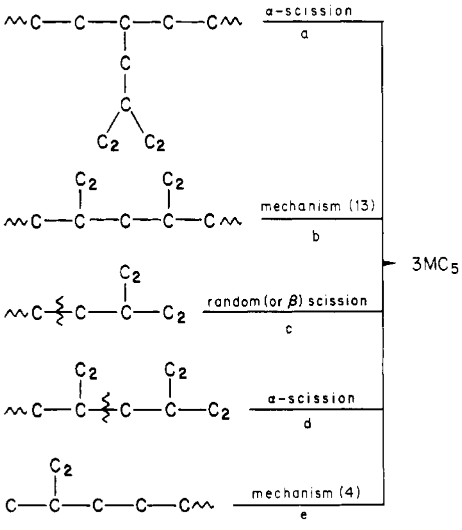

(15)

Of course, there are other compounds formed from these branches and chain ends but of these compounds almost none of them are formed from more than one of these groups. (Pentane, it should be noted, is an exception as it is a favored product—although no more than $3MC_5$—from mechanisms 15a–d. A look at the pyrogram for PE5503 (Figure 11) shows that pentane is indeed in greater abundance than in the pyrograms of the model copolymers.)

Unfortunately, $3MC_5$ is not the only very common scission product. In the enlarged scheme, $3MC_7$ is also a common scission product. Common enough, in fact, that its presence in excess in the pyrograms of the HPPE's can no longer be said to be direct proof of Willbourn branches of the 2-ethylhexyl type. However, since the data and proposed scheme match so well and since 2-ethylhexyl branches are an integral part of that scheme, it would be unreasonable to assume that they do not exist.

The number of branches found in this study is much more numerous than expected. In order to determine the relative concentrations of each type of branch, studies of copolymers with the new types of branches would have to be conducted. Thus the polymerization scheme in Scheme I should be regarded as empirical only. The sensitivity of this technique is obviously very high but no exact quantitative data can be obtained from this study alone.

Conclusions

(1) Low-temperature, low-conversion pyrolysis yields an abundance of fragments from branch points of polyethylene.

(2) The pyrolysis of model copolymers yields only those fragments expected on the basis of the simple α- and β-scission pyrolysis mechanisms.

On the basis of these conclusions and three simple assumptions regarding free radical reactions, a scheme of free radical intramolecular hydrogen transfer mechanisms has been proposed that necessarily conclude the following.

(3) The types of branched pyrolysis products are much more numerous than expected and are best explained by invoking 1,3 intramolecular hydrogen transfer as well as the already familiar 1,5 intramolecular hydrogen transfer.

(4) Both types of Willbourn branches, 2-ethylhexyl and 1,3 ethyl pairs, are prominent products in the proposed intramolecular hydrogen transfer scheme.

(5) The proposed intramolecular hydrogen transfer scheme accounts very well qualitatively for the observed pyrolysis products. However, this study cannot be used along to determine the relative concentrations of the branch structures proposed.

Registry No. *co*((4-Methyl-1-pentene)ethylene), 25213-96-1; *co*((4-ethyl-1-octene)ethylene), 86689-57-8; *co*((5-ethyl-1-nonene)ethylene), 86689-58-9; *co*((1-butene)ethylene), 25087-34-7; *co*((1-butene)(1-octene)ethylene), 28829-58-5; polyethylene, 9002-88-4.

References and Notes

(1) Willbourn, A. H. *J. Polym. Sci.* **1959**, *34*, 569–597.
(2) Dorman, D. E.; Otorka, E. P.; Bovey, F. A. *Macromolecules* **1972**, *5*, 574–577.
(3) Randall, J. C. *J. Polym. Sci., Polym. Phys. Ed.* **1973**, *11*, 275–287.
(4) Cudby, M. E. A.; Bunn, A. *Polymer* **1976**, *17*, 345–347.
(5) Bovey, F. A.; Schilling, F. C.; McCrackin, F. L.; Wagner, H. L. *Macromolecules* **1976**, *9*, 76–80.
(6) Axelson, D. E.; Levy, G. C.; Mandelkern, L. *Macromolecules* **1979**, *12*, 41–52.
(7) Dechter, J. J.; Mandelkern, L. *J. Polym. Sci., Polym. Phys. Ed.* **1980**, *18*, 1955–1961.
(8) Boyle, D. A.; Simpson, W.; Waldron, J. D. *Polymer* **1961**, *2*, 323–340.
(9) Kamath, P. M.; Barlow, A. *J. Polym. Sci., Part A-1* **1967**, *5*, 2023–2030.
(10) Bowmer, T. N.; O'Donnell, J. H. *Polymer* **1977**, *18*, 1032–1040.
(11) Van Schooten, J.; Evenkins, J. K. *Polymer* **1965**, *6*, 561–577.
(12) Michajlov, L.; Zugenmaier, P.; Cantow, H. J. *Polymer* **1968**, *9*, 325–343.
(13) Northmore, B. R. *Br. Polym. J.* **1972**, *4*, 511–525.
(14) Seeger, M.; Barrall, E. M. *J. Polym. Sci., Polym. Chem. Ed.* **1975**, *13*, 1515–1524.
(15) Ahlstrom, D. H.; Liebman, S. A.; Abbas, K. B. *J. Polym. Sci., Polym. Chem. Ed.* **1976**, *14*, 2479–2495.
(16) Liebman, S. A.; Ahlstrom, D. H.; Starnes, W. H.; Schilling, F. C. Third International Symposium on Poly(vinyl chloride), Case Western Reserve University, Cleveland, Ohio, Aug 1980.
(17) Sugimura, Y.; Tsuge, S. *Macromolecules* **1979**, *12*, 512–514.
(18) Roedel, M. J. *J. Am. Chem. Soc.* **1953**, *75*, 6110–6112.

(19) Casey, K.; Elston, C. T.; Phibbs, M. K. *Polym. Lett.* **1964**, *2*, 1053–1056.
(20) Tirpak, G. *Polym. Lett.* **1965**, *3*, 371–374.
(21) Tirpak, G. *Polym. Lett.* **1966**, *4*, 111–114.
(22) Van Dohlen, W. C.; Wilson, T. P. *J. Polym. Sci., Polym. Chem. Ed.* **1979**, *17*, 2511–2527.
(23) Van der Molen, Th. J. *Prepr. IUPAC Conf. (Budapest)* **1969**, *3*, 19.
(24) The following abbreviations are used in the remainder of the paper: $3MC_5$ = 3-methylpentane, $3MC_9$ = 3-methylnonane, $5MC_9$ = 5-methylnonane, etc. These are also used in the chromatograms.

Statistical Mechanical Theory of Deformation of Liquid Crystalline Structure in Styrene–Butadiene Diblock Copolymers in *n*-Tetradecane

Hiroshi Watanabe and Tadao Kotaka*

Faculty of Science, Department of Macromolecular Science, Osaka University, Toyonaka, Osaka 560, Japan. *Received September 15, 1982*

ABSTRACT: When a styrene–butadiene (SB) diblock copolymer is dissolved in a selective solvent such as *n*-tetradecane, which is a good solvent for the B blocks but a nonsolvent for the S blocks, micelles with S cores and B cilia are formed in the system. When the concentration and temperature are above and below the respective critical values, these micelles are arranged on a macrolattice to form a liquid crystalline structure, which exhibits plasticity. The rigidity of the macrolattice before yielding is calculated by a modified diffusion equation, as a result of inhomogeneity in concentration of ciliary B segments in the matrix phase induced by deformation of the macrolattice. When the SB concentration is high, the observed rigidity is proportional to the concentration. On the other hand, when the system is diluted, the observed rigidity is no longer proportional to the concentration but decreases more rapidly. The latter behavior is well simulated by the modified diffusion equation. The temperature dependence of the lattice rigidity is also discussed. The actual SB micelle systems exhibit thermally induced disordering of the macrolattice. However, our calculation assumes a narrow-interphase approximation and cannot predict this transition. A more realistic and complicated calculation is neccesary for the simulation of this thermal transition.

I. Introduction

Solutions of AB-type diblock copolymers in selective solvents, which dissolve only one of the two blocks but precipitate the other, often show peculiar rheology:[1-4] Plastic flow and thixotropy in steady shear flow[1-3] and nonlinear dynamic response due to the plasticity under oscillatory shear strain.[4,5]

In recent studies,[5-7] we examined the rheology of solutions of styrene–butadiene (SB) diblock copolymers dissolved in *n*-tetradecane (C14) and pointed out that the existence of higher order structure or liquid crystalline structure in the solution caused the plasticity and, hence, was responsible for the peculiar rheology. Since the solvent, C14, was a good solvent for the B block but a nonsolvent for the S block, microphase separation occurred and micelles with precipitated rigid S cores and dissolved B cilica were formed in the C14 solution. We call such an SB/C14 solution a "micelle system" in the following discussion. When the SB concentration c exceeded a certain critical concentration $c_R{}^*$ and/or the temperature T was below a certain critical temperature T^*, the SB/C14 solution exhibited plasticity. However, the plasticity disappeared and the system became viscoelastic when c was below $c_R{}^*$ and T was above T^*. Of course, $c_R{}^*$ was dependent on T and T^* was dependent on c. These results[5-7] suggest that the formation of micelles in the solution is not enough but some higher order structure is required so that the micelle system exhibits plasticity.

Detailed small-angle X-ray scattering (SAXS) studies[6-8] revealed that in SB/C14 solutions below $c_R{}^*$ and above T^*, where the solution is viscoelastic, micelles of SB molecules are randomly dispersed in the solution. In those above $c_R{}^*$ and below T^*, where the system exhibits plasticity, these micelles are arranged on a simple cubic (sc) type lattice[6-8] (but *not* on a face centered cubic (fcc) type lattice, which had been assumed to exist). We call this lattice a "macrolattice" in the following discussion.

To describe the morphology of microdomain structure of block copolymers in bulk, where the compressibility is low and inhomogeneous density profiles of the block segments in each domain are strongly inhibited, Meier[9] and Helfand and co-workers[10-12] developed a mean field theory and solved modified diffusion equations under the incompressible limit. Helfand and co-workers[11,12] treated this situation by introducing a potential term that depended on the square of the density deviation divided by the (infinitely) small compressibility into the diffusion equation. As the result, the size and morphology (spherical, cylindrical, or lamellar structure) of the microdomains were determined as a function of composition and molecular weight in such a way that each block chain confined in a microdomain can assume the thermodynamically most stable (optimal) conformation, avoiding those conformations that create density inhomogeneity in the microdomain. They could successfully predict the domain size and shape and the interphase structure.[9-12] Their theoretical predictions were substantiated by Hashimoto and co-workers[13] in their SAXS studies. However, for systems having spherical domains Meier[9] and Helfand and Wasserman[12] employed a spherically symmetric geometry to describe each domain and did not determine what type of packing of the spherical domains would be the most stable one.

Recently, Noolandi and Hong[14] extended the modified diffusion equation approach to block copolymer solutions, taking into account solvent–polymer interactions explicitly. They solved the mean field equation under the constraint of no volume change upon mixing solvent molecules and block segments for lamellar block copolymer structure and investigated the effect of solvent on the size and interphase structure of the microdomains. For the SB/toluene system, in which toluene is a common good solvent for both

0024-9297/83/2216-1783$01.50/0